

Application of Laser Raman Scattering to the Study of Turbulence

DANNY L. HARTLEY*

Sandia Laboratories, Livermore, Calif.

Laser Raman spectroscopy has been utilized as a primary diagnostic technique for transient gas mixing studies. Fluid properties and jet formation have been varied to identify the effects of fluid pressure, jet velocity, jet orifice diameter, and gas specie identity on turbulent mixing rates for one gaseous specie injected into a dissimilar, originally quiescent gas.

Nomenclature

C_1	= proportionality constant
C_2	= proportionality constant
C_{N_2}	= concentration of nitrogen
D^T	= turbulent diffusion coefficient
D_0	= normalizing diffusion coefficient
$D_{N_2, He}^T$	= turbulent diffusion coefficient for N_2 jet into He
k	= turbulent wavenumber
p	= pressure
P_r	= receiver pressure
P_s	= source pressure
P_{r_i}	= initial receiver pressure
r	= radial coordinate
t	= time
T	= time from valve opening until achievement of uniform mixture
V_j	= jet velocity
ν	= kinematic viscosity
ρ	= density

Introduction

A GREAT deal of work has been published on both the turbulent mixing of coflowing jets and jets into a quiescent environment, but very little effort has been devoted to examining what effects the mixing environment (pressure, geometry, and viscosity) has on turbulent gas mixing. This lack of data is partially due to the difficulty in obtaining mixing environments at various pressures in the lab and partially to inadequate techniques of unsteady specie concentration measurement.

However, the author's recent application of laser Raman scattering to the measurement of gas specie concentrations in unsteady flows^{1,2} has now provided a technique to investigate the effects of pressure, viscosity, gas specie, and jet formation conditions on turbulent mixing rates.

This paper concerns application of this technique to the study of these parameters. This work is an extension of the author's earlier experiments in which a given mole fraction of one gas specie was injected into a spherical cavity that contained a dissimilar quiescent gas (see Fig. 1). Temporal and spatial concentration measurements of the injectant gas are obtained to illustrate the rate at which the two gases mixed.

Initial tests in this facility were performed to verify the technique and, as such, involved radial injection of nitrogen into a mixing chamber filled with helium. Stagnation and recirculation of the injectant jet caused gas mixing to occur at a fast rate comparable to the mass addition rate. The Raman detection system was capable of measuring the injectant concentration

history but the effects of mass addition and mass diffusion could not be isolated. These results for radial injection were reported in Ref. 2.

A new injection configuration was devised whereby the injectant gas enters the mixing chamber tangentially. In this configuration, the injectant fills an outer annular region of the mixing chamber and diffuses toward the center as a result of turbulent mixing at the interface. This case proved particularly interesting in that complete mixing was not accomplished until long (several seconds) after the injectant had been introduced; thus it was possible to isolate the jet-dominated mixing rate from the quasi-isotropic equilibrium turbulent mixing rates that occur after jetting ceases. Shadowgraph movies of this configuration were obtained by Johnston.³ These movies clearly illustrate the initial stratification and flow development.

Using the tangential injection configuration, the current series of tests was performed to study the factors that influence turbulent gas mixing rates. The factors studied were: 1) pressure in the mixing chamber; 2) source-to-receiver pressure ratio; 3) injection orifice diameter; 4) injectant gas molecular weight; 5) receiver gas molecular weight; and 6) receiver gas kinematic viscosity. The results of these experiments offer considerable insight into the nature of turbulent mixing and illustrate how individual test parameters or combinations of test parameters can influence mixing rates.

Previous Experiments

Harsha⁴ has published a thorough summary of the theoretical and experimental investigations of steady free turbulent mixing. The reported investigations largely relate to determining centerline velocity decay rates and centerline concentration decay rates for freejets. Zakkay et al.⁵ have measured turbulent diffusion rates for compressible turbulent jets for hydrogen, helium, and argon-air mixtures. In that study, concentration measurements were obtained using thermal conductivity cells. Zakkay concludes that turbulent diffusion rates are directly dependent upon jet centerline velocity, but essentially independent of gas specie identity; he did not consider varying pressure levels.

Some studies, although limited in scope and applicability, have been performed to investigate the effects of the physical environment (artificial turbulence, walls, etc.) on mixing. Fejer⁶ has studied techniques of enhancing turbulent mixing of coaxial streams by varying the jet inlet conditions. He concludes that adding artificial turbulence to the jet or swirling the jet will enhance the mixing rate. He also found that for coflowing streams of dissimilar densities, the centerline velocity and concentration decay were inversely proportional to the axial distance when the inner stream was the more dense and inversely proportional to the square of the axial distance when the inner stream was the less dense. Thus a light gas injected into a heavy gas should mix faster than a heavy gas injected into a light gas.

Received April 19, 1973; revision received December 10, 1973. This work was supported by the U.S. Atomic Energy Commission under Contract AT-(29-1)-789.

Index category: Jets, Wakes, and Viscid-Inviscid Flow Interactions.

* Supervisor, Aerodynamics Division. Member AIAA.

Sheriff⁷ has measured turbulent diffusion rates for air in a circular duct by measuring axial concentration of an injected tracer gas (nitrous oxide). He concluded that turbulent diffusion was proportional to both the mean flow velocity and the duct diameter; however, he did not vary pressure or specie.

Khrastov⁸ measured the effect of pressure on turbulent mixing rates in a combustion chamber. He measured diffusion rates from photographs of the diffusion wake of luminous particles (smoke) behind a point source and determined the dispersion rate of the smoke from the photographs. He concluded that his grid-produced, quasi-isotropic diffusion rates varied proportional to the mean velocity and proportional to the pressure as $D^T = C_1 \bar{V} p^{0.34}$, but that scale of turbulence was independent of pressure.

Semenov⁹ measured the effects of pressure on turbulent mixing rates in a closed container. Semenov artificially generated the turbulence with paddle mixers in a spherical cavity and used velocity fluctuation measurements from an anemometer to deduce relative diffusion rates. He concluded that the diffusion rates in his closed containers were inversely proportional to the pressure as $D^T = C_2 p^{-0.4}$. Semenov's result differs considerably from Khrastov's. However, considering the crude nature of the measurement techniques and the unusual environments for the two experiments, both results are of questionable accuracy.

Experimental Facility

The facility which was used for the radial injection studies of Ref. 2 as well as for the tangential injection studies of this paper is illustrated in Fig. 1. A 6-in. diam spherical mixing chamber has four sapphire windows on orthogonal axes for optical access. Injectant gas is stored in a cylindrical source container that has a free-floating piston. The injectant gas is stored in the experiment side of the cylinder and compressed by loading the piston from the other side by another gas. The source container is connected to the mixing chamber by 0.089-in. i.d. tubing, which is inserted 0.25 in. into the mixing cavity. The end of the tube is sealed and a small orifice (0.020- and 0.040-in. diam for the tests performed) drilled in the side. When the valve is opened, gas is injected tangentially into the mixing chamber where it mixes with the receiver gas.

A 100-kw pulsed, nitrogen laser beam is focused to a 1-mm spot within the mixing chamber. This spot defines a 1-cubic mm sample volume, the location of which may be varied by adjusting the optics. Raman scattered light from the sample volume is collected at 90° by a viewing lens focused into a spectrometer that isolates the Raman shifted wavelengths of light associated with the gases under study. The intensity of each Raman emission line is monitored by a photomultiplier tube and used to determine the concentration of the particular gas in the sample volume. Each laser pulse yields a data point, and thus individual

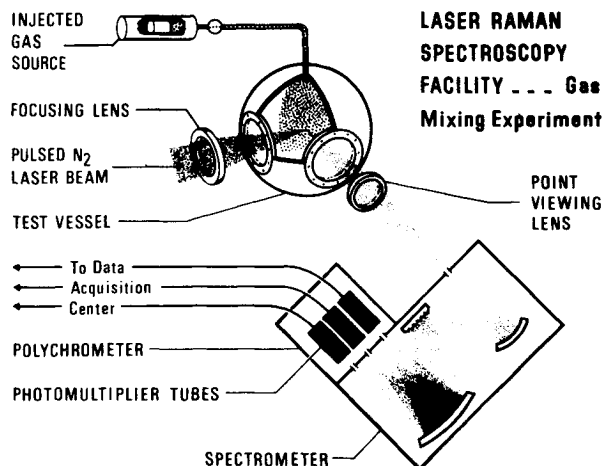


Fig. 1 Laser Raman spectroscopy facility—gas mixing equipment.

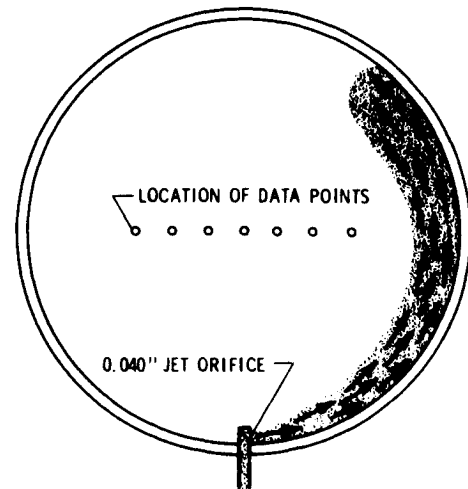


Fig. 2 Tangential injection configuration.

gas specie concentrations at a focus point can be studied as a function of time. Up to 100 data points per second may be obtained using the maximum repetition rate of the pulsed laser. A complete description of the physical equipment and electronic data acquisition system is presented in Refs. 1 and 2.

Basic Tangential Injection Results

The basic tangential injection experiments were performed by initially filling the mixing chamber with 100 psi of helium. An additional 20% mole ratio of nitrogen was then swept tangentially into the chamber from a 500-psi source, filling an outer annular region and causing a forced rotation of the gas in the chamber and subsequent diffusion toward the sphere center. The nitrogen concentration measurements were collected at the sphere center, 0.5, 1.0, and 1.5 in. radially outward from the center. The location of these data points is shown approximately in Fig. 2.

In Fig. 3, which presents the nitrogen concentration measurements obtained at the center of the sphere, two distinct mixing rates are identifiable. During the gas injection phase, i.e., from valve opening ($t = 0$) until pressure equilibrium ($t \approx 2.0$ sec), the injectant concentration at the sample point increased rapidly and

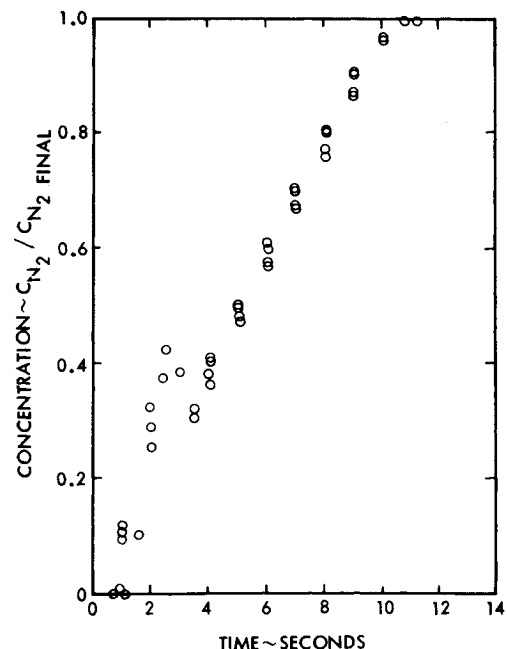


Fig. 3 Nitrogen concentration vs time for tangential injection into helium, $r = 0$.

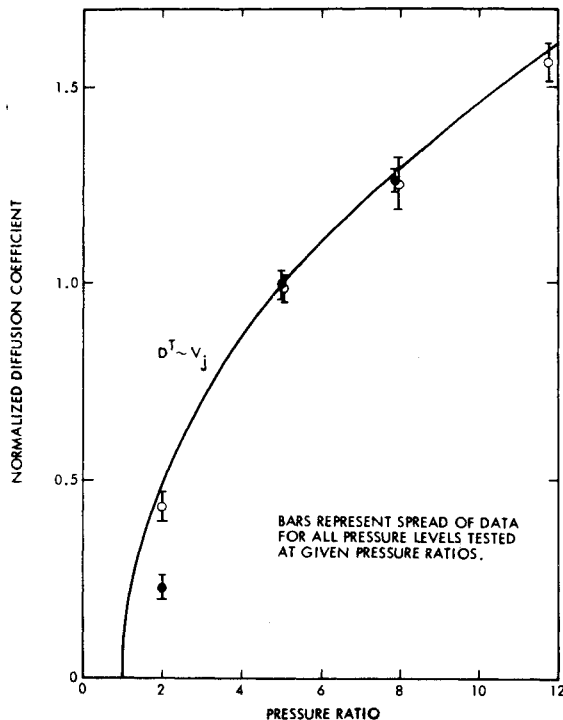


Fig. 4 Normalized diffusion coefficient measurements for early-time mixing rates as a function of pressure ratio (velocity). Nitrogen tangentially injected into helium.

nearly linearly. This early-time mixing rate is dictated by the incoming jet and the turbulence it generates. After the jet flow ceases, the early-time mixing rate persists for a short time and then decays to a lower late-time mixing rate. According to Hinze,¹¹ this behavior is analogous to turbulent eddy interaction behind a grid where an initial and final period of turbulence can be identified. During the initial period of decay, the flow velocities and thus Reynolds numbers are high. As a result, the distribution of turbulent eddy sizes is inertia-dominated, with a uniform (for all eddy sizes) decay rate which is a function of the fluid kinematic viscosity. Decreasing the fluid kinematic viscosity correspondingly reduces the decay rate such that the early-time mixing rates should persist even longer. However, for later times, the Reynolds number decreased (fluid motion slows), and the turbulence distribution becomes more viscosity dominated. This condition corresponds to the final period of turbulence defined by Hinze. For low Reynolds numbers, the smaller eddies are preferentially dissipated by viscosity and the larger eddies, which cause turbulent diffusion, exhibit a large degree of permanence. The small eddies, which dissipate the turbulence, are essentially independent of the condition of formation but are dependent upon the kinematic viscosity.

An over-all mixing time of 10.5–11 sec is evident from the results shown in Fig. 3. Data obtained from points 1.0 and 1.5 in. from the sphere center exhibit similar behavior.

In summary, the early-time mixing rate should be formation dependent (jet velocity dependent) and independent of fluid properties. However, the decay of the early-time mixing rate, or persistence after jetting ceases, is dependent on the fluid kinematic viscosity. The late-time mixing rate, in contrast, should be independent of the condition of formation but the mixing rate itself is directly dependent upon the fluid kinematic viscosity. Further discussion of these turbulence interaction effects is given later in this paper.

The fact that the present physical geometry is not amenable to exact analytical treatment is of limited consequence in this paper since it is the relative (not absolute) values of diffusion rates caused by changes in test parameters that are important. Thus for the purpose of this paper an effective diffusion rate will be presented which is deduced from the rate of change of

injectant concentration and normalized to the diffusion rate of the early stage of the basic tangential injection case (Fig. 3).

Effect of Pressure Ratio on Mixing Rates

The pressure at which the nitrogen is injected into the helium in the mixing chamber was varied to allow for source-to-receiver pressure ratios of 2.0, 5.0, 8.0, and 11.8. These pressure ratios were repeated for all chamber pressures and gas pairs tested. The result of increasing the pressure ratio for a fixed value of receiver pressure is to: 1) increase the total momentum in the jet, and 2) reduce the jet-on time. Since the same amount of injectant mass is input for all values of pressure ratio, the increased jet momentum is reflected as an increase in jet velocity. The effect of increasing the jet velocity is to increase the intensity of turbulence and, as a result, significantly increase the diffusion rates. Several studies have been reported in the literature^{4,5} which illustrate the linear dependence of turbulent diffusion rates on jet velocity for turbulent jets in quiescent environments and for coflowing jets.

For the unchoked cases, the jet velocity (momentum) may be related to pressure ratio by the incompressible Bernoulli Equation to give¹³

$$V_j \sim [(P_s/P_r) - 1]^{1/2} \quad (1)$$

Assuming that⁵

$$D^T \sim V_j$$

then

$$D^T \sim [(P_s/P_r) - 1]^{1/2} \quad (2)$$

For increased pressure ratios (> 2) the flow chokes at the jet orifice and forms an underexpanded jet until the jet adjusts to the ambient pressure. Even for the underexpanded jets, however, the effective diffusion rates appear to behave according to Eq. (2).

Figure 4 presents the early-time mixing rates as a function of pressure ratio. Using the linear velocity dependence for turbulent diffusion adequately predicts the difference in measured diffusion rates for $P_s/P_r = 2, 5, 8$, and the limited data at $P_s/P_r = 11.8$. However, in the case of the smaller orifice, the experimental results for $P_s/P_r = 2$ are lower than might be expected because the jet-on time approaches the minimum obtainable mixing time and further increases in jet-on time, such as is achieved with a smaller orifice, only serve to prolong final equilibrium mixing.

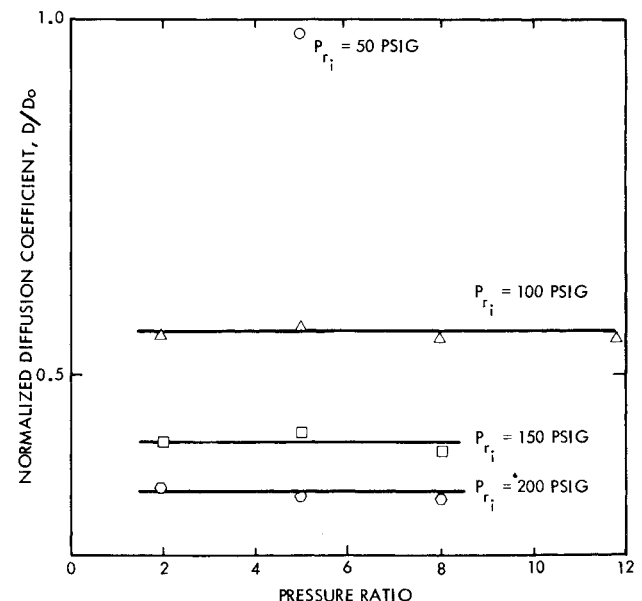


Fig. 5 Normalized turbulent diffusion coefficient measurements for late-time mixing rates as a function of pressure ratio. Nitrogen tangentially injected into helium.

Figure 5 presents the results for late-time mixing rates for the various pressure ratios. In contrast to the early-time results, the late-time rates appear to be independent of the pressure ratio, and thus independent of the original jet condition. Assuming the late-time turbulence to be quasi-isotropic, the flow is then analogous to low Reynolds number (slow mean flow velocities) isotropic turbulence, as defined by Hinze. The eddy distribution for such turbulence is influenced by fluid properties but is independent of the condition of formation.

Effect of Fluid Pressure on Mixing Rates

The mixing chamber pressure was varied from 50 to 200 psig while retaining fixed values of pressure ratio and injectant mole fraction. As shown in Fig. 6, the early-time rates are inertia-dominated and characteristic of jet properties only and are not affected by increased fluid pressure. However, after the jet ceases, these jet-dominated rates persist until the existing nonisotropic turbulence can decay to the late-time quasi-isotropic turbulent structure. This decay rate is a function of kinematic viscosity, which is the primary mechanism of eddy interaction and momentum dissipation. Thus increasing the pressure or decreasing the kinematic viscosity allows the early-time rates to persist longer. The importance of this latter effect is discussed in a later section.

Figure 7 presents the results for late-time mixing rates for the various pressures. Here, the late-time rates appear to be independent of the original jet conditions, but are strongly influenced by the mixing chamber pressure. If one assumes that the late-time flow is quasi-isotropic, then this behavior can be explained on the basis of Hinze's¹¹ discussion of turbulent energy distribution and eddy interaction. That is, for increased pressure (decreased kinematic viscosity) more of the energy is transferred to the large wave-number region (smaller eddies), thus reducing the scale of turbulence represented by mean eddy size. The low-wave number, large eddies are primarily responsible for turbulent mass diffusion; therefore, the result of increasing pressure for a field of isotropic turbulence is to reduce the mixing rate. Similarly, according to Hinze, this low Reynolds number case represents an eddy distribution which should be independent of the condi-

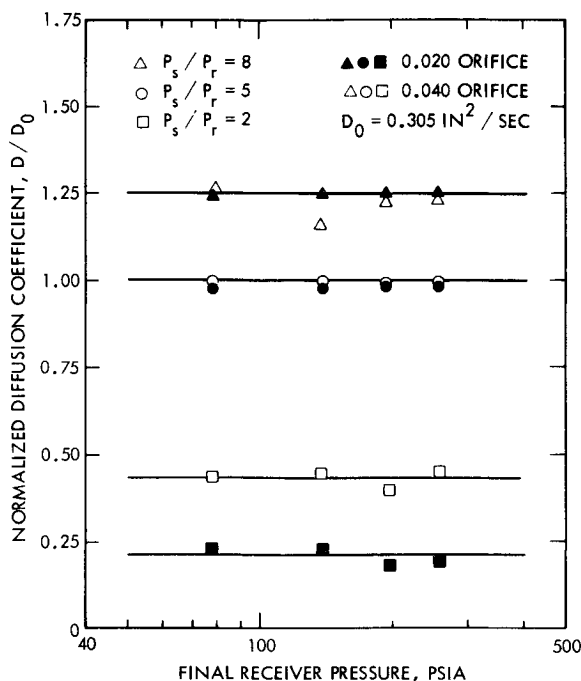


Fig. 6 Normalized diffusion coefficient measurements for early-time mixing rates as a function of final receiver pressure. Nitrogen tangentially injected into helium.

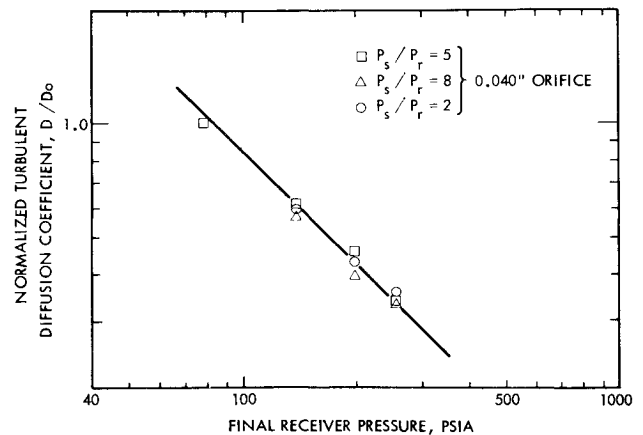


Fig. 7 Normalized turbulent diffusion coefficient measurements for late-time mixing rates as a function of receiver pressure. Nitrogen tangentially injected into helium.

tion of formation. This conclusion is consistent with the present results.

Khramstov⁸ measured the variation of the scale of turbulence behind a grid with changing pressure and concluded that it was independent of pressure. Khramstov's data proved to be unexpected, since he had assumed that with a drop in pressure the scale of turbulence would grow, due to an increase in kinematic viscosity, and this should result in the disappearance of small-scale eddies and a corresponding increase in the mean scale of turbulence. His expectations, however, were based on the assumption that he had measured diffusion in a viscous-dominated isotropic turbulent field. Batchelor and Townsend¹⁴ have shown that the "final period" of turbulence behind a grid, where viscosity dominates, exists only beyond 500 mesh diam downstream. In regions nearer the grid, "initial period" exists where the turbulence is inertia dominated. Since Khramstov's measurements were obtained in the first 10 mesh diam downstream from the grid, his results should reflect inertia rather than viscous effects. In that sense his measurements of the scale of turbulence near the grid are analogous to and consistent with the present results for "early-time" mixing rates, which were found to be independent of pressure.

On the other hand, Semenov⁹ measured the effects of pressure on turbulent mixing rates and concluded that turbulent diffusion was inversely proportional to pressure. He measured fluctuations in artificially generated turbulence using several paddle wheels in a container. In the absence of any global velocities, he was measuring a quasi-isotropic turbulence characteristic of viscous-dominated "final period" or "late-time" turbulence, which is inversely proportional to pressure to some power. His results, as he notes, did not agree with the measurements by Khramstov⁸; however, he should not have expected agreement since dominant effects in the two studies were so different. Thus the trend of Semenov's data agrees with the present results for "late-time" turbulence, and Khramstov's data trend agrees with the present results for "early-time" turbulence.

Effect of Orifice Size on Mixing Rates

For the configuration tested in this study, the injection orifice is the principal flow control mechanism, with the flow being choked at the orifice. Thus, knowing the source pressure and temperature, the flow properties at the orifice can be calculated from isentropic flow relations. For fixed pressure and pressure ratio, the flow velocity and density at the orifice are independent of the orifice diameter as long as the flow is choked. Thus decreasing the orifice diameter only changes total mass flow rate, not velocity, and prolongs the early-stage mixing process. Figure 6 shows how the change in orifice diameter from 0.040 to 0.020 in. affected the measured early-time mixing rates. For pressure

ratios of 5 and 8, the reduced orifice had no effect on the early-time rates, but for a pressure ratio of 2, the mixing rate was significantly lower for the smaller orifice. However, for the low-pressure ratio case the mass injection time approached the minimum obtainable mixing time; any further decrease in mass flow rate makes final equilibrium mixing become a function of mass addition rather than mass diffusion. The most significant conclusion is that an optimum orifice diameter exists such that early-time mixing rates are unaffected but are caused to last longer.

Effects of Combined Parameters

Three parameters have been identified which have been shown to significantly influence the turbulent mixing of two gases in an enclosed container. These parameters are the pressure, the source-to-receiver pressure ratio, and the jet orifice diameter. The previous sections have discussed how each of these parameters can affect the turbulence behavior during "early-time" jet mixing as well as during "late-time" quasi-isotropic mixing. However, it is the combination of both stages of mixing that accomplishes a final equilibrium mixture and establishes a mixing time for a particular configuration. Thus a particular mixing time can be tailored (minimized if so desired) by properly choosing parameters.

By studying the combined effects of parameter variations it becomes evident that for certain combinations both early and late-time mixing rates are enhanced; for some combinations both are degraded; and for some combinations one is enhanced and one is degraded. The latter case is the most probable combination, and thus optimization of mixing times becomes a complex operation. The transition from one type of mixing combination to another is not a clear-cut phenomenon, but the trends caused by various combinations of design parameters can be identified in the experimental results. In Fig. 8, actual mixing times are presented for the case of nitrogen injected tangentially into helium through a 0.040-in.-diam orifice. A monotonic increase in mixing time with increased pressure is evident from the results. However, this simple monotonic behavior no longer exists when the orifice diameter is reduced as illustrated in Fig. 9. Figure 9, which presents the equilibrium mixing times for nitrogen injected into helium through the 0.020-in.-diam orifice, illustrates the complex effects that design parameters can have on mixing times. Specifically, the reduced orifice size can increase mixing times in some cases or can decrease mixing times in other cases.

Parameters can, therefore, be varied such that mixing occurs in a minimum time or tailored to a specific longer mixing time. This control on design performance can have significant effects on combustion chamber or propulsion system designs.

Changes in Gas Specie

Changing Injectant Gas Specie

The injectant gas was changed from nitrogen to other non-toxic diatomic gases to observe molecular weight effects. Hydrogen and deuterium were used as injectant species, retaining

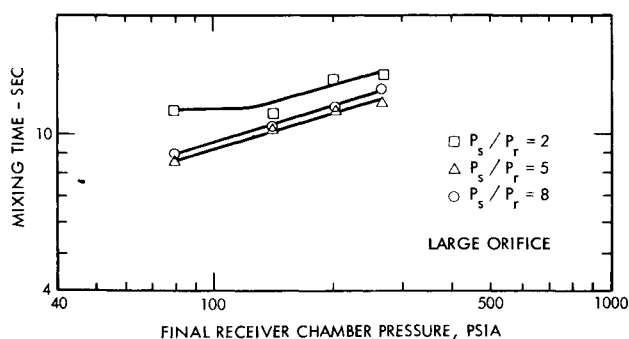


Fig. 8 Gas mixing times for nitrogen injected into helium for various pressures and pressure ratios using the larger orifice.

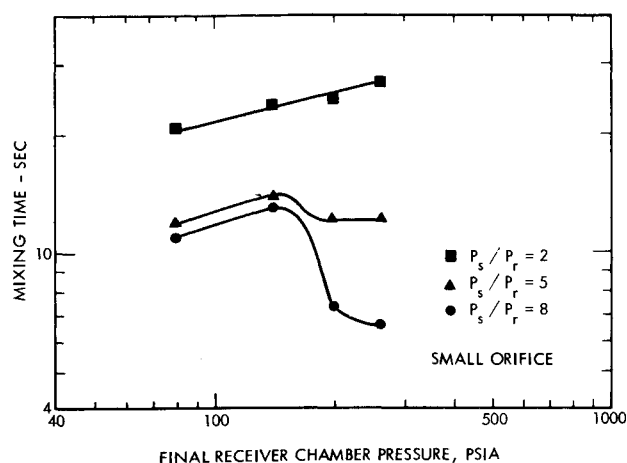


Fig. 9 Gas mixing times for nitrogen injected into helium for various pressures and pressure ratios using the smaller orifice.

helium as the receiver gas. These light injectant gases yield a strong vibrational Raman signal at a wavelength far from the Rayleigh line. This change in injectant molecular weight from nitrogen also offers a large change in sound speed and jet velocity, thus amplifying the effects of injectant molecular weight on turbulent gas mixing. Source-to-receiver pressure ratios of 2 and 5, initial receiver pressure levels of 100 and 200 psig, and orifice diameters of 0.020 and 0.040 in. were tested. The over-all mixing times for these tests are presented in Fig. 10. For all cases, increasing the pressure ratio decreased mixing times as before, but, unlike the nitrogen/helium cases, increasing the receiver pressure always reduced mixing times. This latter result implies that the over-all flow is more inertia dominated, with most of the mixing occurring during the early-time process. This trend is understandable since, for the same source-to-receiver pressure ratio, the jet velocity will vary inversely with the molecular weight. Since the nonisotropic, jet-dominated mixing rate is directly proportional to the jet velocity, the early-time mixing rates for hydrogen and deuterium jets should be much higher than for a nitrogen jet and thus accomplish much of the mixing before the jet turbulence decays. Since this makes early-time mixing rates dominate, increasing pressure should reduce mixing time (as it does).

Not only did the hydrogen- and deuterium-helium cases mix much faster than the nitrogen-helium cases, but the hydrogen-helium case mixed faster than deuterium-helium by a factor of

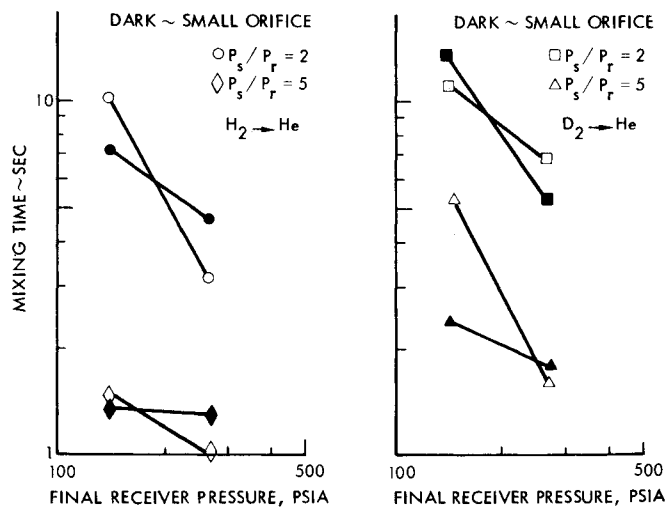


Fig. 10 Gas mixing times for changed injectant gas species.

nominally one and a half. This result again illustrates the domination of early-stage mixing rates where mixing varies with jet velocity, which, for sonic orifices, varies with the square root of inverse molecular weight (1.414 for deuterium vs hydrogen). Departures from this molecular weight effect occurs only for cases where mixing takes longer and late-time turbulence becomes important.

The effects of changing orifice size is also shown in Fig. 10. As discussed earlier, the variation in orifice size has compounding effects—principally: 1) prolonging the early-time mixing rate such that viscous dissipation of jet turbulence becomes important; and 2) decreasing the net mass flow rate such that total mixing becomes dependent upon mass influx rather than mass diffusion. The complexity of these counter-acting effects is evident from the results in Fig. 10 and is not clearly resolved.

Changing Receiver Gas Specie

The receiver gas was changed in an effort to identify the role played by that gas in the over-all mixing process. The cases tested and compared are shown in Table 1. All were done at a 200-psig initial receiver pressure, a pressure ratio of 5.0, and an orifice diameter of 0.040 in.

Table 1 Mixing times for various receiver gases

Case	Injectant specie	Receiver specie	Mixing time (sec)
A-1	H ₂	He	1.00
A-2	H ₂	D ₂	0.75
B-1	D ₂	He	1.60
B-2	D ₂	H ₂	4.00

In case A, using hydrogen as an injectant, the receiver gas was changed from helium to deuterium. Both helium and deuterium have the same molecular weight, and thus no change due to inertial effects was expected. However, deuterium has a kinematic viscosity which is 30% smaller than that for helium. Hence early-time mixing, which was shown to dominate for the hydrogen injection cases studied, was predicted to persist longer when deuterium was the receiver gas; this prediction was verified by the results of case A.

In case B, using deuterium as the injectant, the receiver gas was changed from helium to hydrogen. Helium and hydrogen have almost identical kinematic viscosities but their molecular weights are significantly different. Hence any observable change in mixing time should result from inertial differences and not viscosity effects. The test results indicate that reducing the molecular weight of the receiver gas (all else remaining constant) by a factor of 2.0 increased the over-all mixing time by slightly more than a factor of 2.0. Townsend¹⁵ examined a simple turbulent flow model in an extensive study of the mechanism of entrainment in free turbulent flows. Using the properties of the entrainment mechanism, he shows that the entrainment rate for a jet increases with increased ambient-to-jet density ratio. However, understanding of this phenomenon and of the part played by various turbulent eddies in the entrainment of ambient fluid is still very incomplete. A similar trend is seen in Fejer's data⁶ for coflowing streams of different densities, but he offers no explanation. However, both results are consistent with all the cases shown in Table 1.

To illustrate the combined effect of viscosity and molecular weight, it is interesting to compare case A-2 with case B-2. At first glance, these cases merely exchange roles of injectant and receiver gas for the two gases, hydrogen and deuterium, and one might expect very little change in mixing times. However, in case A-2 the combined effects of: 1) lighter injectant gas increasing

jet velocity; 2) lower viscosity receiver gas prolonging early-stage mixing rates; and 3) heavier receiver gas being less easily displaced result in the gases mixing five times faster than in case B-2.

Conclusions

For the case of one gas injected tangentially into an enclosed volume containing a dissimilar gas, it was found that over-all mixing was achieved through a two-phase mixing process. The first phase of mixing occurs while the jet is on and persists for a time after the jet ceases. The remaining turbulent mixing is achieved by the quasi-isotropic turbulence that exists after the early-time jet-dominated mixing decays. The early time mixing rates were found to be proportional to the jet velocity but independent of fluid pressure and jet orifice size. The time over which the early-time rate persists, however, is a function of fluid pressure, or kinematic viscosity, and the orifice diameter. In contrast, the late-time mixing rate was found to be inversely proportional to fluid pressure but independent of jet formation conditions.

The resulting over-all time required to obtain a homogeneous mixture within the mixing chamber was found to be related to the various tested parameters in such a way that an optimum combination of pressure, pressure ratio, and orifice diameter may exist for a given gas pair and gas mole fraction ratio such that mixing times can be either maximized or minimized.

References

- ¹ Hartley, D. L., "Unsteady Multispecie Gas Mixture Concentration Measurements Using Laser Raman Scattering," *Proceedings of SPIE 15th Technical Symposium*, Anaheim, Calif., Sept. 1970.
- ² Hartley, D. L., "Transient Gas Concentration Measurements Utilizing Laser Raman Spectroscopy," *AIAA Journal*, Vol. 10, No. 5, May 1972, p. 687.
- ³ Johnston, S. C., "Stability of Rotating Stratified Fluids," *AIAA Journal*, Vol. 10, No. 10, Oct. 1972, p. 1372.
- ⁴ Harsha, P. T., "Free Turbulent Mixing: A Critical Evaluation of Theory and Experiment," AEDC Rept. TR-71-36, Feb. 1971, Arnold Engineering Development Center, Tullahoma, Tenn.
- ⁵ Zakkay, V., Krause, E. F., and Woo, S. D. L., "Turbulent Transport Properties for Axisymmetric Heterogeneous Mixing," *AIAA Journal*, Vol. 2, No. 11, Nov. 1964, p. 1939.
- ⁶ Fejer, A. A., Hermann, W. G., and Torda, T. P., "Factors that Enhance Jet Mixing," Rept. 69-0175, Oct. 1969, Aeronautical Research Labs., Wright-Patterson Air Force Base, Ohio.
- ⁷ Sheriff, N. and O'Kane, D. J., "Eddy Diffusivity of Mass Measurements for Air in Circular Duct," *International Journal of Heat and Mass Transfer*, Vol. 14, No. 5, May 1971, p. 697.
- ⁸ Khramstov, V. A., "Investigation of Pressure Effect on the Parameters of Turbulence and Turbulent Burning," *Seventh International Symposium on Combustion*, Butterworths, London, 1959, p. 609.
- ⁹ Semenov, E. S., "Measurement of Turbulence Characteristics in a Closed Volume with Artificial Turbulence," *Combustion, Explosion, and Shock Waves*, Vol. 1, No. 2, 1965, p. 83.
- ¹⁰ Hartley, D. L., "An Experimental Study of Factors that Influence Turbulent Gas Mixing Rates," Rept. SCL-RR-720034, Jan. 1973, Sandia Labs., Livermore, Calif.
- ¹¹ Hinze, J. O., *Turbulence*, McGraw-Hill, New York, 1959.
- ¹² Kee, R., "A Finite Difference Algorithm for Spherical Polar Coordinates," Rept. SCL-DR-720017, Aug. 1972, Sandia Labs., Livermore, Calif.
- ¹³ Shapiro, A. H., *The Dynamics and Thermodynamics of Compressible Fluid Flow*, Vol. 1, Ronald Press, New York, 1953.
- ¹⁴ Batchelor, G. K. and Townsend, A. A., "Decay of Isotropic Turbulence in the Initial Period," *Proceedings of the Royal Society*, London, 193A, 1948, p. 539.
- ¹⁵ Townsend, A. A., "The Mechanism of Entrainment in Free Turbulent Flows," *Journal of Fluid Mechanics*, Vol. 26, Pt. 4, 1966, pp. 689-715.